DEM-based structural mapping: examples from the Holy Cross Mountains and the Outer Carpathians, Poland

ANDRZEJ KONON & MICHAŁ ŚMIGIELSKI

Institute of Geology, University of Warsaw, Al. Żwirki i Wigury 93, PL-02-089 Warszawa, Poland
Email: Andrzej.Konon@uw.edu.pl; M.Smigielski@uw.edu.pl

ABSTRACT:

KONON, A. & ŚMIGIELSKI, M. 2006. DEM-based structural mapping: examples from the Holy Cross Mountains and the Outer Carpathians, Poland. *Acta Geologica Polonica*, **56** (1), 1-16. Warszawa.

The study of the Earth's surface using DEM-generated products combined with geological maps or satellite and aerial photographs provides information that is very useful for structural analysis. Applications of shaded-relief images, slope, openness, and aspect maps, 3D terrain views, profiling, contouring and semiautomatic intersections to selected parts of the Holy Cross Mountains and the Bieszczady Mountains are shown. The analysis led to the discovery of transverse faults in both fold and thrust belts, determination of the components of movement along these faults and the courses of the Łysogóry fault zone and the Dukla thrust fault. The application of these methods also enabled the display of changes in shape profiles of map-scale folds such as the Niewachlów anticline and the Baligród syncline.

Key words: Digital Elevation Model, Derivatives of DEM, Folds, Faults, Holy Cross Mountains, Bieszczady Mountains.

INTRODUCTION

Identification of geological structures including folds and faults, based on surface morphology, is helpful for preparing or revising surface structural maps. Progress during the last decade in the applications of a new tool, digital elevation modelling, enables a detailed analysis of the spatial distribution of faults and the geometry of folds. Processing digital elevation models (DEMs) is useful in showing landforms (e.g. KÜHNI & PFIFFNER 2001; MILIARESIS & ILIOPOULOU 2004), identifying the fold patterns and structural style in deformed stratigraphical packages (BANERJEE & MITRA 2005), analysis of block movements (COLLET & *al.* 2000), discovering active faults (e.g. OGUCHI & *al.* 2003; CHEN & *al.* 2004; SUNG & CHEN 2004; GANAS & *al.* 2005) and analysis of slope movements (IWAHASHI & *al.* 2001). DEMs are also used in mapping the distribution and shapes of volcanoes (ADIYAMAN & *al.* 1998), as well as measuring the bedding strike and dip (BANERJEE & MITRA 2005). DEM-based morphometry has been also applied to the identification and measurement of fault scarps (e.g. HOOPER & *al.* 2003; GANAS & *al.* 2005), calculations of fault slip rates (GANAS & *al.* 2005), estimations of amounts of dip-slip fault movements (WALKER & JACKSON 2002) and recognizing the phases of tectonic uplift (RIQUELME & *al.* 2003; BOOTH-REA & *al.* 2004). Progress in space investigations also allowed the use of DEMs derived from the Mars orbiter laser altimeter to characterize Martian topography (OKUBO & *al.* 2004).

In this study, different analytical methods of DEMs combined with the techniques of remote sensing images, geological maps and field observations are applied to discover tectonic structures. Apart from the commonly used DEM-generated maps like shaded relief images, slope maps, aspects maps and openness maps are also tested. DEM has also been used in the construction of 3D terrain views.

Fig. 1. Location of the Holy Cross Mountains (A) and the Bieszczady Mountains (B) displayed on the shaded-relief image (sun direction 335°, sun elevation 35°, 10 × vertical exaggeration) obtained from GTOPO30 DEM

Parts of the Holy Cross Mountains (HCM) and the eastern part of the Polish Outer Carpathians (EPOC) have been selected for analysis (Text-fig. 1). In the HCM, preliminary analyses of DEMs have been carried out in their southern part (KONON & *al.* 2004) and in the Outer Carpathians a study of the Vsetínske Vrchy Mountains was made (BíL 2003). In both the regions investigated, there are regional fault-related folds built of unmetamorphosed sedimentary rocks of different ages (Text-figs 2-3) and mechanical properties. The folds are cut by faults, which developed during or after the folding with dip-slip and/or strike-slip components. DEMs in these fold belts, together with geological maps and field observations may provide new useful information about the details of the geometry of structures and the location of the fault zones.

GEOLOGICAL SETTING

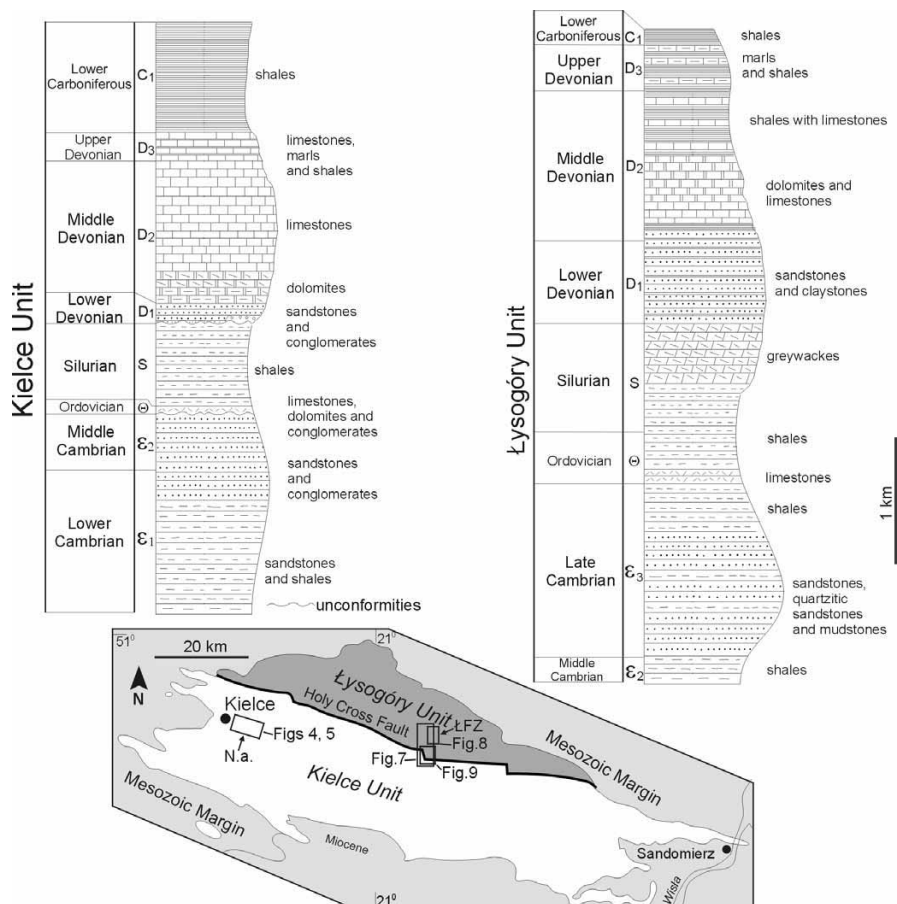For the analysis, five regions from the Holy Cross Mountains and the Outer Carpathians (Text-figs 2-3)

Fig. 2. Geological sketch-map of the Holy Cross Mountains (after KSIĄŻKIEWICZ & *al*. 1965) with location of the selected study areas (N.a. – Niewachlów anticline, ŁFZ – Łysogóry fault zone) and lithostratigraphic columns for the Kielce and Łysogóry units (based on HAKENBERG 1973, ORŁOWSKI 1975, STUPNICKA 1992 – and references therein, slightly simplified). For other explanations see text

have been selected where, based on digital processing of DEMs, it was possible to provide new data or to revise details of the different structures such as folds and/or faults.

Holy Cross Mountains (HCM)

The Holy Cross Mountains consist of a Palaeozoic massif, traditionally termed the Palaeozoic core, including the Łysogóry (northern) and Kielce (southern) tectono-stratigraphic units (CZARNOCKI 1919; POŻARYSKI 1978). They are located within the Trans-European Suture Zone (BERTHELSEN 1993). The HCM fold belt consists of a series of 100-120° trending, fault-related folds, built up of Lower Cambrian to Lower Carboniferous rocks (CZARNOCKI 1938). Based on the mechanical properties of the rocks, the Palaeozoic succession can be divided into relatively competent and incompetent packages. The competent packages are represented by Upper Cambrian and Lower Devonian quartzitic sandstones, Ordovician and Middle-Upper Devonian dolomites, limestones and siliciclastic shales (Text-fig. 2). Data on the currently investigated rocks

point to their tensile strength ranging from 5 to 7 MPa and, in the case of the Lower Devonian and Cambrian sandstones, up to 18 and 20 MPa respectively (PINIŃSKA 1994). The incompetent packages, represented by Cambrian, Silurian and Carboniferous shales and thin-bedded sandstones, were not laboratory tested but their strengths are significantly weaker. These rocks in the Łysogóry and Kielce units were folded after the Viséan, as a result of Variscan deformations (CZARNOCKI 1919, 1957) due to N-S to NNE-SSW shortening (e.g. LAMARCHE & al. 1999).

Eastern part of the Polish Outer Carpathians (EPOC)

The Outer Carpathians fold-thrust belt forms a northwardly convex zone, about 1000 km long and up to 100 km wide, which comprises Upper Jurassic to Lower Miocene rocks, mainly unmetamorphosed sediments (e.g. OSZCZYPKO 2004). The folding and thrusting proceeded during Late Oligocene and Miocene times due to the convergence of the European plate with ALCAPA (ROYDEN 1988; OSZCZYPKO & ŚLĄCZKA 1989; PLAŠIENKA & al. 1997). After this phase the uplift of the Outer Carpathians
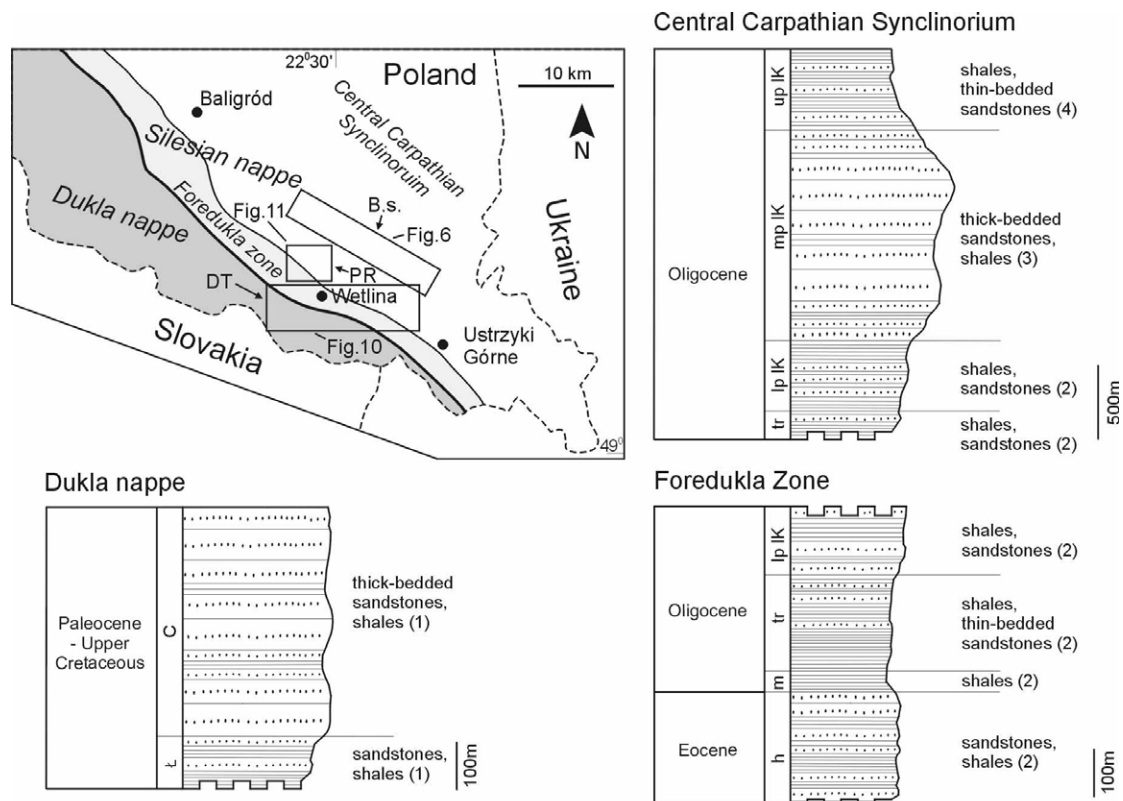

Fig. 3. Geological sketch-map of the Bieszczady Mountains with location of the selected study areas (B.s. – Baligród syncline, DT - Dukla thrust, PR - Połoniny range) and lithostratigraphic columns from selected areas of the Dukla Nappe, the Central Carpathian Synclinorium and the Foredukla Zone (based on ŚLĄCZKA & ŻYTKO 1979; ŚLĄCZKA 1980; WDOWIARZ 1985; RUBINKIEWICZ 1996 – and references therein, slightly simplified). For other explanations see text

began (KSIĄŻKIEWICZ 1972; FODOR & *al.* 1999). The area of the EPOC investigated includes the Silesian Nappe, composed of the Foredukla Zone and the Central Carpathian Synclinorium separated by thrust zones (KSIĄŻKIEWICZ 1977), as well as a small segment of the Dukla Nappe (Text-fig. 3). In this region, the segment of the Carpathian fold-thrust belt consists of 110-135° trending fault-related folds cut by strike-slip and/or normal faults (ŚLĄCZKA & ŻYTKO 1979; WDOWIARZ 1985; ŚLĄCZKA & KAMIŃSKI 1998). The folds are built up of Lower Cretaceous to Palaeogene rocks (ŚWIDZIŃSKI 1958; ŚLĄCZKA 1971). Based on the mechanical stratigraphy, this rock complex can be divided into four main structural packages in ascending order: (1) a lower complex consisting of relatively competent Upper Cretaceous – Palaeocene sandstones with shales; (2) a package comprising mainly incompetent Eocene-Oligocene shales; (3) a package of competent Oligocene thick-bedded sandstones and (4) an upper package consisting of a relatively incompetent interlayered sequence of Oligocene shales and sandstones (SIKORA 1959; ŚLĄCZKA 1980) (Text-fig. 3). Data on the currently investigated typical sandstones sampled in the Outer Carpathians point to their tensile strength ranging from about 5 to 13 MPa (PINIŃSKA 2003). The incompetent packages are significantly weaker. The whole rock sequence was folded and thrusted in Miocene times as a result of SSW-NNE shortening (e.g. OSZCZYPKO 2004).

METHODS

Our analysis was based on digital processing of DEMs for the HCM and EPOC, with a ground resolution of 50×40m and 20×30m respectively. DEM derivatives such as elevation maps, slope maps, aspect maps, shaded relief images (reflectance maps), openness maps and 3-D terrain images have been analysed. Moreover, some of these derivatives were merged to create combined images. All the maps and images were made using the MICRO-DEM/TerraBase II software series created by PETER GUTH, and Surfer, version 8.0, Golden Software.

Slope and aspect maps

Aspect and slope are properties of a plane tangent to a point on a surface. The aspect is an azimuth of a slope line (line of locally greatest rate of altitude change). The slope is the angle between the slope line and the horizontal plane.

There are many algorithms that compute slope and aspect, and numerous studies have reported their precision (i.e. HODGSON 1998; JONES 1998; ZHOU & LIU 2004). To calculate slope and aspect values, the second

order finite difference algorithm by FLEMING & HOFFER (1979) method was used. This algorithm ensures the best accuracy of the derived parameters (JONES 1998; ZHOU & LIU 2004). The slope and aspect values were estimated in a three by three grid window as a local property of DEM and then assigned to the central cell of the window. In this way the aspect and slope angles were computed for each grid cell.

Values of slopes have been presented on maps as the sine of their angle or in degrees, the aspect as the value of its azimuth. Slope map-generated contours enable a precise location of structures. To avoid mistakes in interpreting slope maps, especially when the slope angles change only slightly, strongly contrasting colour scales have been applied.

Shaded-relief images

Shaded-relief images show the local orientation of the surface in relation to the defined light source direction (YOELI 1965). Morphological features that are almost parallel to the defined light source are faint, whereas those that lie at almost 90° to the light direction become enhanced (COOPER 2003). For that reason, a different azimuth and a different elevation of the light source were used in this study to generate shaded-relief images. Vertical exaggeration of the given surface enhanced the whole shading effect, showing more topographic details. In order to estimate the reflectance value in each grid cell, the aspect and slope angles have been computed. Reflectance was calculated afterwards with the use of the Lambertian reflection method (e.g. HORN 1982) and the algorithm of PELTON (1987).

Shaded-relief images are similar to radar images showing bare-ground surfaces without vegetation (e.g. OGUCHI & *al.* 2003) and display relationships between the topography and geology. They enable the discovery of contacts between individual rock sequences with different mechanical properties.

Openness maps

Openness at a grid point is a parameter that describes the mean morphology around that point (YOKOYAMA & *al.* 2002). Positive and negative openness maps can be derived from DEM. A positive openness value is high for convex forms, whereas a negative openness value is high for concave forms. Openness maps, similar to shaded relief maps, enhance features of the topography but are independent of the position of the light source (YOKOYAMA & *al.* 2002). Openness maps enable direct observation of regional structures and preliminary control of the intersection lines. Precise location of struc-

tures, similarly as on the slope maps, is possible, based on openness map-generated contours.

The present work tests positive openness maps. Openness was computed as the mean value of zenith angles measured in eight compass directions up to the L distance (YOKOYAMA & *al.* 2002, figs 1 and 3). The choice of L highlights the topography at a different scale, therefore L 500 m and L 1000 m openness maps have been used. Tones of grey were assigned to values of openness, whereas white was reserved for the highest value of this parameter.

3-D terrain images, merging, semiautomatic intersections and profiling

In order to generate 3-D terrain models, satellite images from Landsat 7 were draped over the DEMs. Landsat 7 provides seven-band images. The present paper employed the ETM+ orthorectified, compressed mosaics comprising bands 2 (visible green light), 4 (near-infrared light) and 7 (mid-infrared light). The ETM+ image has an effective resolution of 14.25 m. 3D terrain views enable

observations of structures from different directions and with different values of exaggerations. Precise determination of the geometry of folds or location of faults is restricted by distortions resulting from perspective.

Geological maps (CZARNOCKI 1938; ŚLĄCZKA & ŻYTKO 1979) were geo-rectified and merged with shaded relief images. Moreover, colour-scaled elevation maps were merged with shaded relief images and airphotos at 1:10 000 scale in order to obtain more refined mapping of morphological features.

For precise analysis of attitudes of structural planes on the elevation maps, intersection lines have been computed. This very quick and precise method enables the analysis of parameters of any structural planes over vast areas, where tectonic activity occurred.

In order to display the changes in shape profiles of folds and analyse the fault scarps, elevation profiles showing topography were extracted from the DEMs. The profiles were made along selected lines in the case of folds sub-perpendicular to their axes, and sub-perpendicular to contours in the case of scarps.
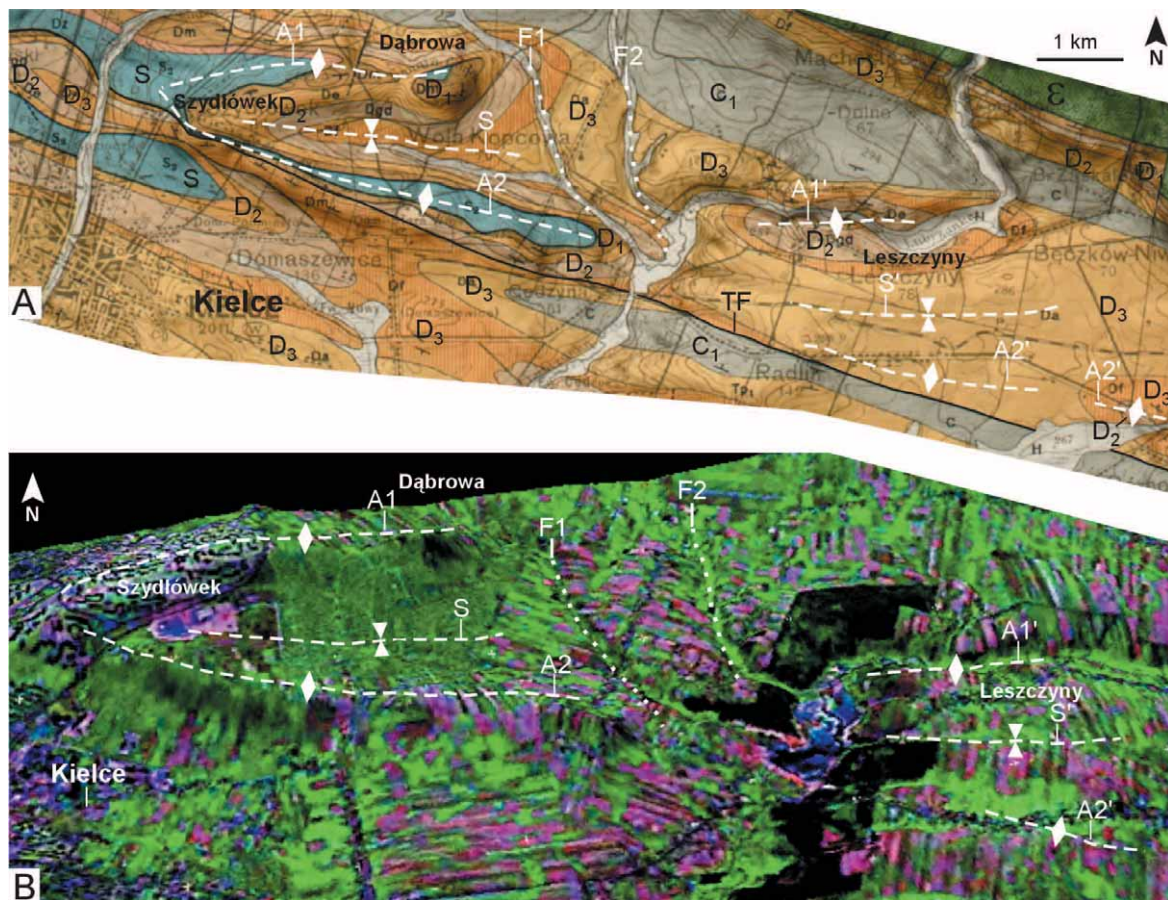

Fig. 4. DEM-products of the Niewachlów anticline (A) Geological map (CZARNOCKI 1938) merged with shaded-relief image (sun direction 335°, sun elevation 35°, 10 × vertical exaggeration). A1, A2, A1', A2' – anticlines, S, S' – synclines, F1, F2 – transverse faults, TF – thrust fault. (B) 3D terrain model of the Niewachlów anticline looking north (7 × vertical exaggeration). For other explanations see Text-fig. 2 and tex

DEM-BASED ANALYSIS FOR STUDY SITES

Folds

Niewachlów anticline

The Niewachlów anticline (CZARNOCKI 1919) is an example of a fold with different shape profiles along its axis. This 90-105° trending anticline comprises an incompetent rock complex consisting of Lower and Middle Cambrian shales alternating with thin-bedded sandstones, and Silurian shales with intercalations of greywackes; and a more competent rock complex consisting of Lower Devonian sandstones, conglomerates, shales and Middle-Upper Devonian carbonate rocks (CZARNOCKI 1938, 1956; FILONOWICZ 1973a, b) (Text-figs 2, 4). According to the field observations of FILONOWICZ (1973a), the western part of the anticline near Niewachlów is asymmetric and south-vergent, with an overturned, faulted southern limb dipping at 70-80° and a northern limb dipping at 35-45° (Text-figs 5A and B – I). Our analysis based on DEM derivatives shows that in the central part, near Szydłówek, the shape profile of this fold clearly changes. The 3D terrain view and shaded-relief image clearly display two hills connecting at Szydłówek, separated by a valley (Text-figs 4B, 5A). The shaded-relief image merged with the geological map of CZARNOCKI (1938) show that these hills are built mainly of competent Lower Devonian clastic sandstones, and the slopes are composed of Silurian shales with greywackes (Text-fig. 4A). The valley, particularly eastwards, is filled with less competent Middle
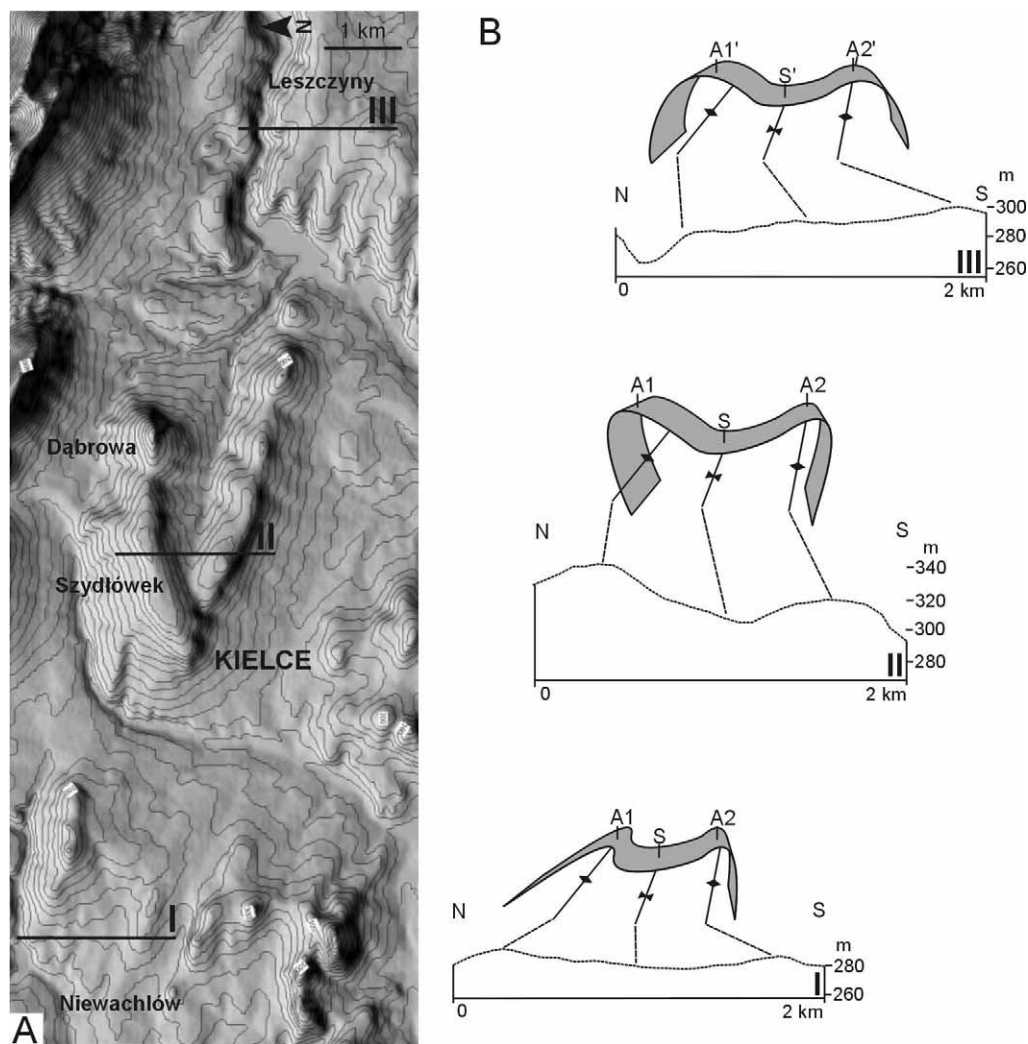

Fig. 5. Shape profiles of the Niewachlów anticline. (A) Shaded-relief image (sun direction 335°, sun elevation 35°, 10 × vertical exaggeration) with contours and elevation profiles lines I, II and III. (B) Elevation profiles (10 × vertical exaggeration) with simplified shape profiles of the fold (attitudes of fold limbs after CZARNOCKI 1956; FILONOWICZ 1969, 1973a). For other explanations see text

and Upper Devonian rocks (Text-fig. 4A). Hence, this DEM derivative suggests that the hinge zone of the first-order fold comprises two anticlinal branches (A1 – northwards, A2 – southwards), connecting in the western part, and one subsidiary syncline (S) (Text-figs 4, 5A, B – II). This indicates that the anticline in this region is a fan-shaped fold (Text-fig. 5B – II), which can be confirmed by the geological cross-section of CZARNOCKI (1956, pl. 12).

CZARNOCKI (1957) suggested a continuation of the Niewachlów anticline further to the east. The DEM-derived images (Text-fig. 4) also confirm the possibility of a continuation of the fold in this direction as a fan fold (KONON & al. 2004). In the east, near Leszczyny and Górno, the same pattern of folds occurs repeatedly two A1' and A2' anticlines, separated by an S' syncline, corresponding to the A1, A2 anticlines and the S syncline respectively (Text-figs 4, 5A, B – III). The geological map (CZARNOCKI 1938), merged with the shaded-relief image and the 3D terrain view, also shows the occurrence of the A1', A2', S' fold axes further to the south in relation to the axes of the A1, A2 anticlines and the S syncline (Text-fig. 4). This probably resulted from their offset along NW-SE trending transverse F1, F2 faults (Text-figs 4A, B) that were not identified by CZARNOCKI (1938) and FILONOWICZ (1973a, b). The strike separations across these faults are up to 2 km. Small differences in the widths of the hinge zone of this fold near Dąbrowa and Leszczyny suggest the evidence for the mainly dextral strike-slip components and probably dip-slip component on the transverse faults (Text-fig. 4A). The faults cut the fold and presumable terminate at the TF fault (Text-fig. 4A) (CZARNOCKI 1938, 1956), which suggests either that they post-date the Variscan folding or that they developed in the late phase of this tectonic activity.

Variations in the geometry of the Niewachlów anticline from the west, where the fold has an asymmetric geometry (Text-figs 5A, B – I), to the east, where the fan-shape geometry prevails (Text-fig. 5A, B – II, III), suggest, according to criteria of MITRA (2003), that the fold underwent shortening by significantly different amounts.

Baligród syncline

The Baligrod syncline between the Wetlinka River and the Wołosaty stream is a fault-related fold that shows variation in the geometry (Text-fig. 6). The limbs of this fold are built of thick-bedded sandstones of the Lower Krosno Beds, but more incompetent strata occur in the hinge zone (ŚLĄCZKA & ŻYTKO 1979) (Text-figs 3, 6A). The syncline is therefore expressed morphologically as two opposed ridges separated by a valley parallel to the

fold axis (Text-fig. 6). The openness map and 3D terrain view show that the valley is wider in the south-eastern segment of the study area and relatively narrow in its central and north-western part (Text-figs 6B-C). This suggests that in this area the fold axis plunges to the south-east as previously described by ŚLĄCZKA (1980) and WDOWIARZ (1985) or that the fold underwent more shortening in the western part.

DEM-derived images clearly show a change in the geometry of the shape profiles of the fold from west to east. The curving of the ridge lines near transverse stream valleys due to the intersection between the bedding and the terrain surface suggest that the fold geometry turns rapidly between the Hylaty and Prowcza streams (Text-figs 6B, C-D). The intersection indicates that, along the z-z' section, the northern limb of the Baligród syncline dips to the south and, along the z'-z" section, to the north (Text-figs 6B-C). A similar fold geometry was previously suggested by ŚLĄCZKA & ŻYTKO (1979) and MASTELLA (1995). DEM analysis confirms these suggestions and enables the precise location of the area of distinct change in fold vergence. From point z', the syncline in the western part of the study area is an almost symmetrical, upright fold, whereas in the eastern segment it is an asymmetric, south-vergent, overturned fold.

The southern slope of the northern ridge corresponds to the overturned limb of the Baligród syncline. This limb has a step-like profile east of the Prowcza stream (Text-figs 6C-D). The steep parts of this slope are marked by thick-bedded sandstones and the less inclined parts are marked by more incompetent interlayers (TOKARSKI 1975). This morphology enabled an estimation of the strike and dip of the overturned fold limb using semi-automatically computed intersection lines (Text-fig. 6D). The best fit intersection line indicates that, over the entire area between the Prowcza stream and the eastern slopes of the Magura Stuposiańska Mt., the bedding dips 38° to the north and strikes at 123° (Text-fig. 6D). The estimation of bedding parameters was confirmed by strike and dip measurements made by one of us (M.Ś) from outcrops in a nearby stream.

Faults

Łysogóry fault

The Łysogóry fault is an approximately N-S trending, transverse, steeply dipping fault which cuts Cambrian, Ordovician, Silurian and Devonian strata in the Łysogóry Unit (CZARNOCKI 1950, 1957) and possibly also part of the Kielce Unit (KSIĄŻKIEWICZ & SAMSONOWICZ 1953; PAWŁOWSKI 1965; MIZERSKI 1982). The dextral strike-slip

component as well as the dip-slip component (CZARNOCKI 1950; JAROSZEWSKI 1973, fig. 7; 1980, fig. 227) occurred on this fault. According to MIZERSKI (1982) solely the dip-slip component occurred on this fault.

The Łysogóry fault has a wide damage zone. Both in the northern and southern parts, near the Łysogóry range, this zone includes series of faults (CZARNOCKI 1957, fig. 26; FILONOWICZ 1966, 1968) and, near Chełmowa Mt., probably also extension fractures, which could be interpreted as wing cracks, horsetail fractures, or as

antithetic faults (JAROSZEWSKI 1980; DADLEZ & JAROSZEWSKI 1994).

Slope, openness and shaded-relief images, partly with contours, strongly emphasize the differences in resistance to weathering between the competent Devonian and incompetent Ordovician-Silurian rocks in the northern part of the Łysogóry fault zone (Text-figs 7-8). These DEM derivatives show that the 140° trending eastern margin of the mountain (a-a'), north of Bostów, the 140° trending valley of the northern trib-
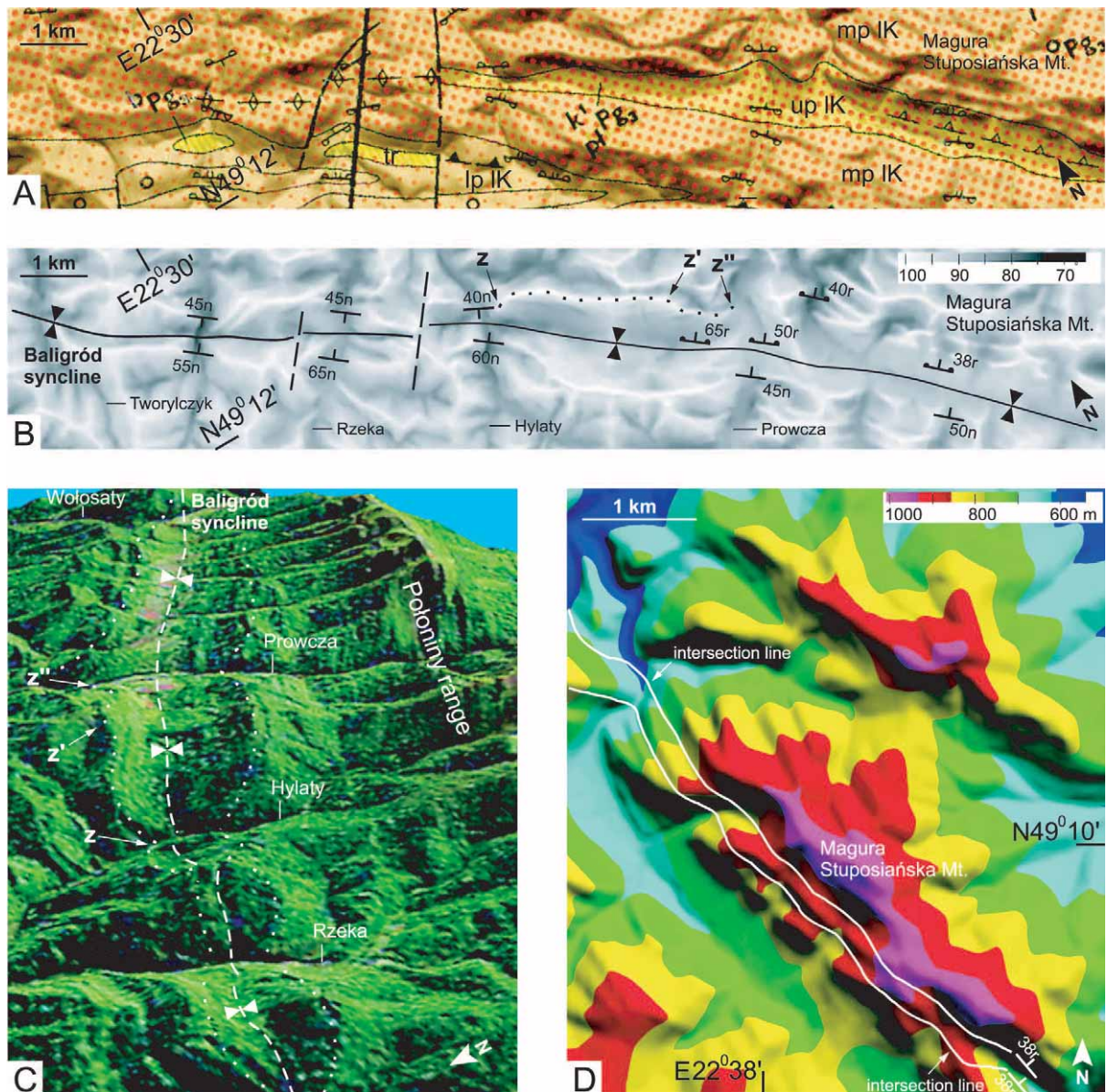

Fig. 6. DEM-products of the Baligród syncline. (A) Geological map (ŚLĄCZKA & ŻYTKO 1979, Łupków Sheet at 1 : 200, 000 scale) merged with shaded-relief image (sun direction 45°, sun elevation 60°, 3 × vertical exaggeration). (B) Positive openness map (L = 500m) with bedding orientation (n – normal, r – reverse), dashed line marks faults, z-z'-z'' segments of the ridgeline. (C) 3D terrain model of the Baligród syncline looking south-east, dotted line marks ridges. (D) Elevation map merged with the shaded-relief image (sun direction 45°, sun elevation 45°, 2 × vertical exaggeration) with intersection lines of bedding planes and bedding orientation (r – reverse). For other explanations see Text-fig. 3 and text

utary stream of the Pokrzywianka river (b-b'), the 35° trending western (c-c') and 25° trending eastern (d-d') margins of the Chełmowa Mt. are almost linear (Text-fig. 7) and transverse in relationship to the bedding (CZARNOCKI 1957). The occurrence of linear landforms is confirmed by the radar image of e.g. the Chełmowa Mt. region (Text-fig. 8B). The margins of the hills with slope angles up to 20° are from a few hundred metres to 3 km long (Text-fig. 7A). Geological maps show that along the margins strata of different ages are in contact (CZARNOCKI 1957). This suggests that they correspond to scarps of the steeply-dipping faults recognized by CZARNOCKI (1957). All of the faults, apart from the fault located along the d-d' scarp, belong to the main Łysogóry fault zone. The fault located along the d-d' scarp (Text-fig. 8C) is probably included in the group of branch faults of this fault zone.

The analysis show that the trends of the inferred faults change in the area between Bostów and Chełmowa Mt. This suggests that the northern part of the main Łysogóry fault zone is distinctly curvilinear, which is confirmed by the field investigations of CZARNOCKI (1950, 1957). According to CZARNOCKI (1957, fig. 26), the change in trend of the fault trace was from 160 to 20°, slightly less than that identified by us from DEM derivatives.

The differences between the competent/incompetent rocks, identified from DEM-generated images, enabled the recognition of similar linear landforms near the Łysogóry range, where Cambrian and Ordovician-Silurian rocks are in contact (Text-figs 7, 9). Slope and openness maps with contours show the occurrence of east-facing linear scarps, sub-perpendicular to the bedding strikes, on the western slopes of the Łysogóry range
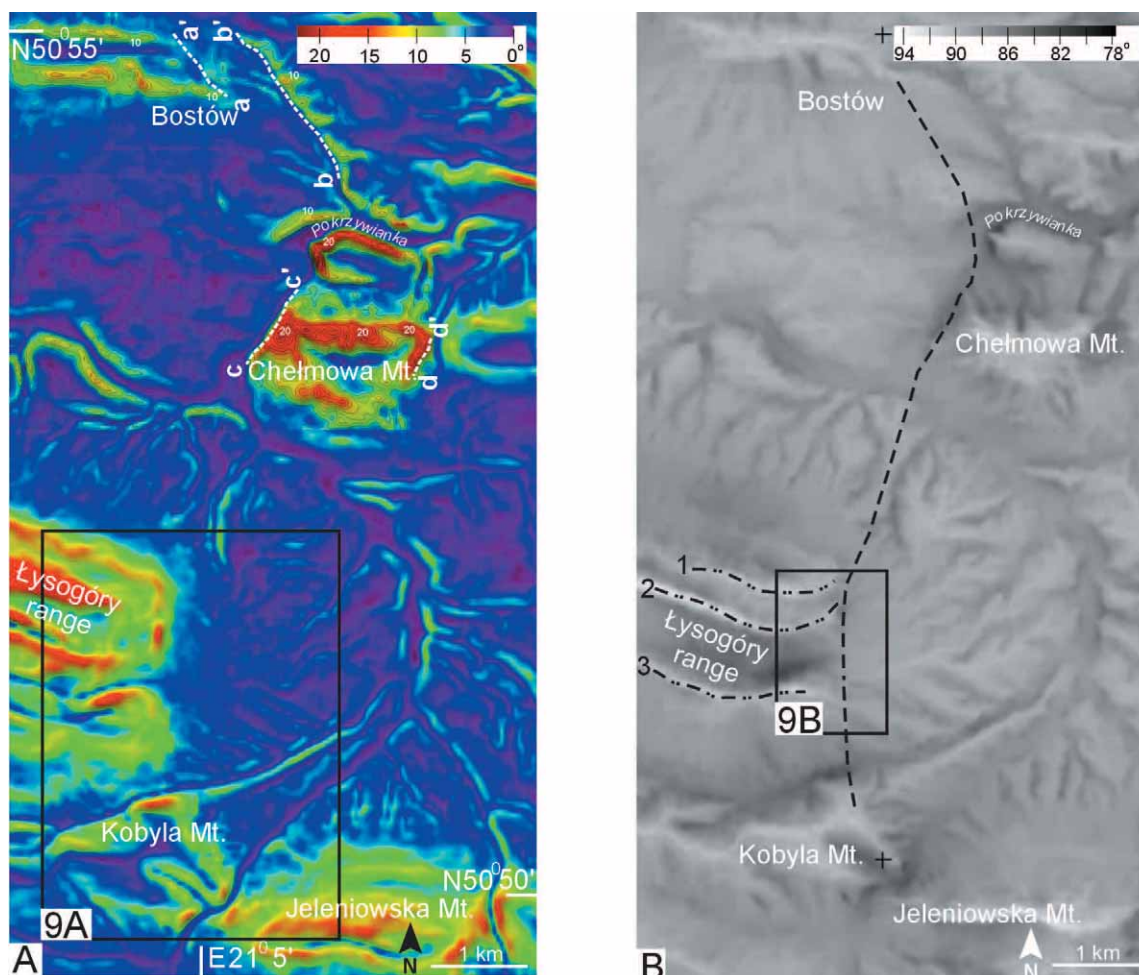

Fig. 7. The DEM derivatives of the Łysogóry fault zone. (A) Slope map (values of slopes presented in degrees) merged with shaded-relief image (sun direction 335°, sun elevation 35°, 10 × vertical exaggeration), northern part with contours and marked fault scarps (a-a', b-b', c-c', d-d'). (B) Positive openness map (L = 1000m) with trace of the Łysogóry fault (dashed line) (according to CZARNOCKI 1957, fig. 28, slightly simplified) and ridges in the Łysogóry range (1, 2, 3). For other explanations see text

and Kobyla Mt. (Text-figs 7, 9). In the northern part, the e-e' scarp is probably located along a N-S trending fault, whereas in the southern part the f-f' and g-g' scarps lie along 155° trending faults (Text-fig. 9A).

The existence of one of these inferred faults is confirmed by a change in bedding attitudes. On the western side of the e-e' scarp of the Łysogóry range, the beds strike at 107°, whereas on the eastern side they strike at about 85° (FILONOWICZ 1966). This fault zone can be found on the elevation profiles through the determination of the place where the slope angles change across the slope (Text-figs 9B-C).

These newly discovered faults are probably either segments of the main Łysogóry fault zone or they belong to the group of steep-dipping faults that prevail in this region (CZARNOCKI 1957), presumably forming a group of branch faults according to the terminology of KIM &

al. (2004). Possibly in this region these faults border the main Łysogóry fault zone from the west.

Analysis of the faults based on DEM derivatives shows that the trend change in the trace of the main Łysogóry fault zone, from the Łysogóry range (180°) to Kobyla Mt. (155°) is slightly greater than that suggested by CZARNOCKI (1957, fig. 26). Both changes – in the northern and southern segment of the analysed Łysogóry fault zone – probably resulted from refraction of the main fault trace during propagation of the fault through rocks of strongly differing competency.

Slope and openness maps (Text-figs 7, 9A) show also that the distance between the Łysogóry range and the Jeleniowska Mt., corresponding to the strike separation across the Łysogóry fault, is about 3.1 km. This is consistent with the value of 3.25 km, calculated by CZARNOCKI (1957).
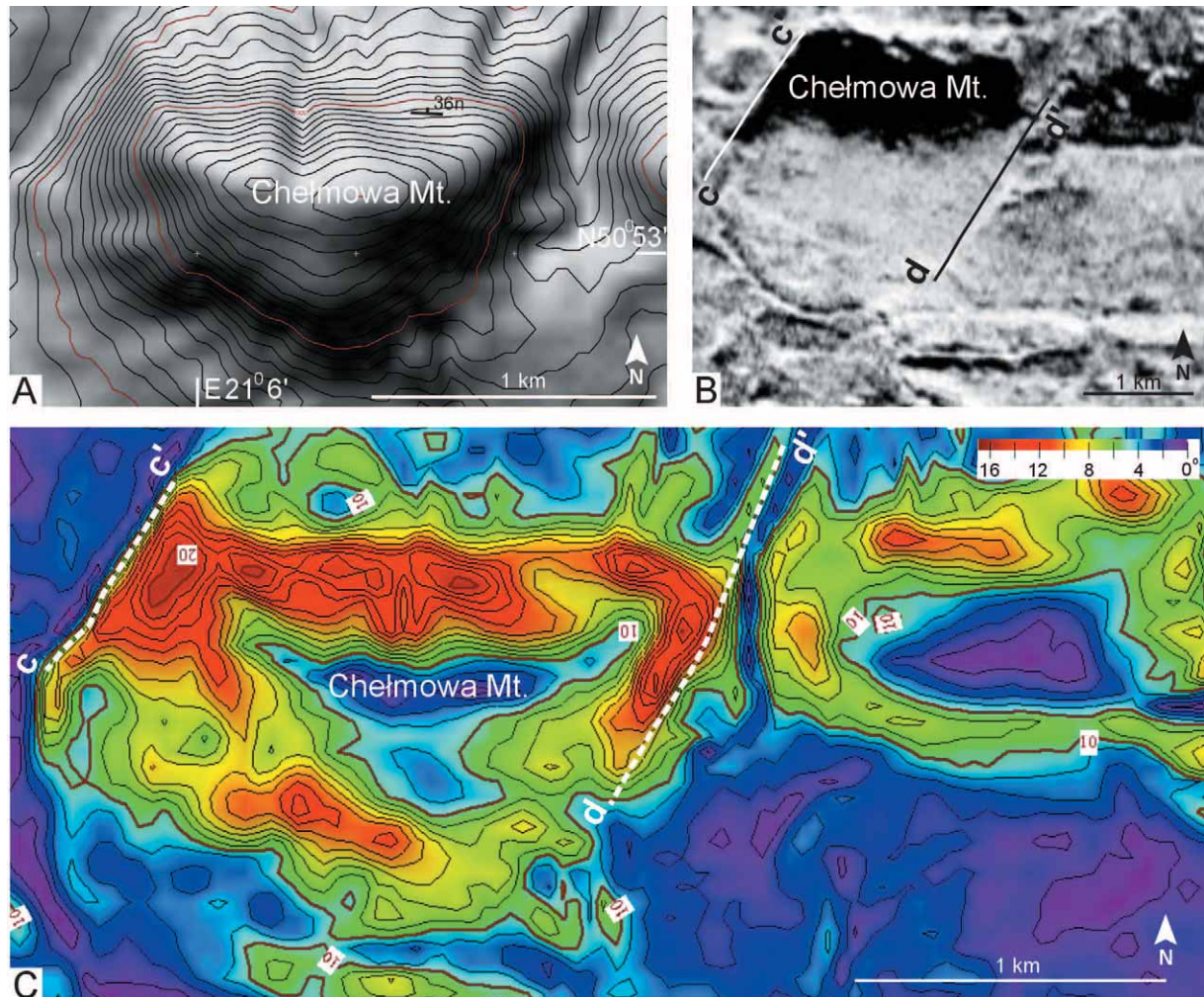

Fig. 8. The DEM derivatives of the Chełmowa Mt. region. (A) Shaded-relief image (sun direction 335°, sun elevation 35°, 10× vertical exaggeration) with contours and bedding orientation (n – normal). (B) Radar image with fault scarps (c-c', d-d'). (C) Slope map (values of slopes presented in degrees) with contours and fault scarps (c-c', d-d'). For other explanations see text
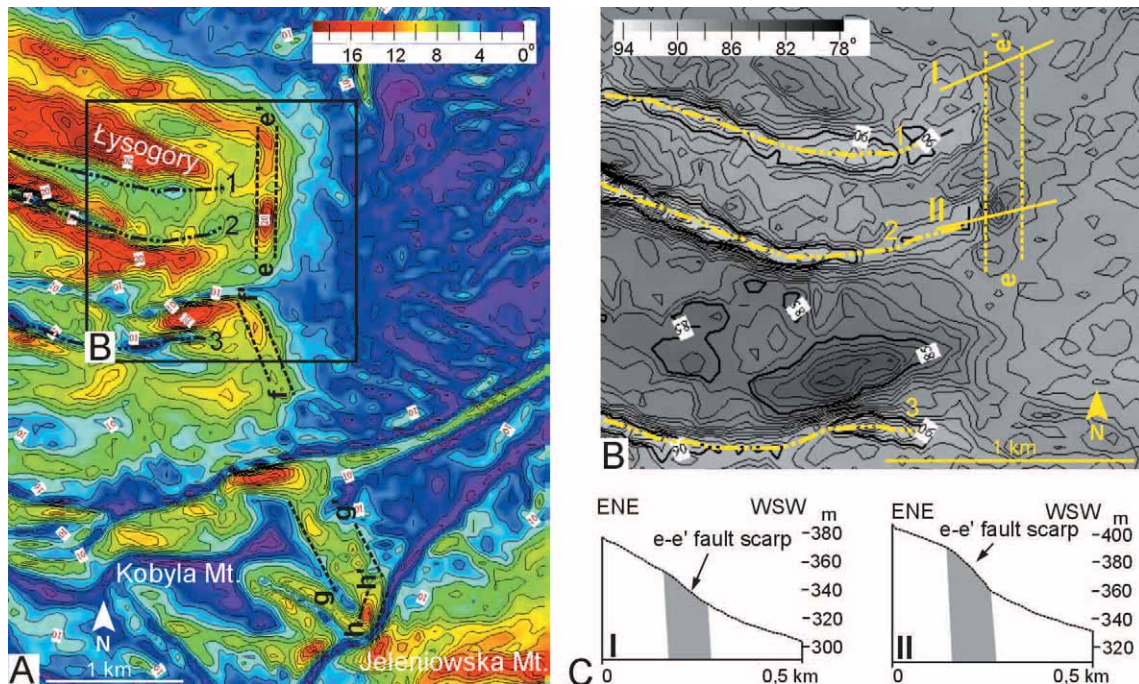
Fig. 9. (A) Slope map (values of slopes presented in degrees) of the Łysogóry range and Kobyla Mt. region, with contours and fault scarps (e-e', f-f', g-g', h-h'). (B) Positive openness map (L = 1000m) of the eastern end of the Łysogóry range with e-e' fault scarp. I, II elevation profile lines. (C) I, II elevation profiles (4 × vertical exaggeration) with e-e' fault zone (grey colour). For other explanations see text

Dukla thrust

The main thrust zone that separates the Dukla nappe and the Silesian nappe strikes at NW-SE and dips at 45°-70° to the SE (ŚWIDZIŃSKI 1958; RUBINKIEWICZ 1996). In the area of Wetlina, the strike of this thrust changes locally to W-E (ŚLĄCZKA & ŻYTKO 1979) (Text-fig. 10A). Along the Dukla thrust fault, the Oligocene Transitional and Lower Krosno Beds of the Foredukla Zone are overlain by Upper Cretaceous Cisna and Łupków Beds of the Dukla nappe (ŚLĄCZKA 1971) (Text-figs 3, 10A). In the study area, the Cisna and Łupków Beds rock complex is composed of thick- to medium-bedded sandstones with shales, whereas the Transitional and Krosno Beds comprise mainly shales and thin-bedded sandstones (RUBINKIEWICZ 1996).

Due to the significant difference in the current mechanical properties between these complexes (Text-fig. 3), the thrust zone is clearly visible on the slope map and 3D image (Text-figs 10B-C). This reflection in topography confirms the earlier field investigations of STARKEL (1969) and TOKARSKI (1975). The slope map and elevation profiles show that a rapid increase in the slope angle values can be observed from NE to SW across the thrust zone (Text-figs 10B, D). The rapid change in the slope angle resulted from the difference between the competent rock complex of the Dukla nappe, which builds the steeper slope, and the incompetent rock complex of the Foredukla Zone, which builds the less steep slopes (Text-fig. 3). The course of the thrust zone derived from DEM compares well with the field observations of ŚLĄCZKA & ŻYTKO (1979), MASTELLA (1995) and RUBINKIEWICZ (1996), but may be more precise along highly inaccessible sections without good-quality exposures between transverse streams.

Fault near Orłowicza Niżna pass - Połoniny range

The Ustrzyki Górne syncline (TOKARSKI 1975) between Wetlina and Ustrzyki Górne is an asymmetric, south-vergent, overturned fold with an almost horizontal axis (ŚLĄCZKA 1980; MASTELLA 1995). In the study area the syncline is composed of competent, thick-bedded Oligocene sandstones of the middle part of the Lower Krosno Beds (ŚLĄCZKA 1980). In the south-western limb of this syncline, secondary folds and longitudinal faults occur (KUŚMIEREK 1979; MASTELLA 1995). The north-eastern, overturned limb of this fold forms the Połoniny range (Text-fig. 11A). Beds in this limb strike at 125° and dip at 45°-65° to the NE (MASTELLA 1995). The ridge has the same direction as the bedding strike and trend of map-scale fold axes, although offsets of the ridge occur locally. One of the zones (x-x') is located on the Orłowicza Niżna pass (Text-fig. 11B) and has a left-hand strike separation of up to 200 m.
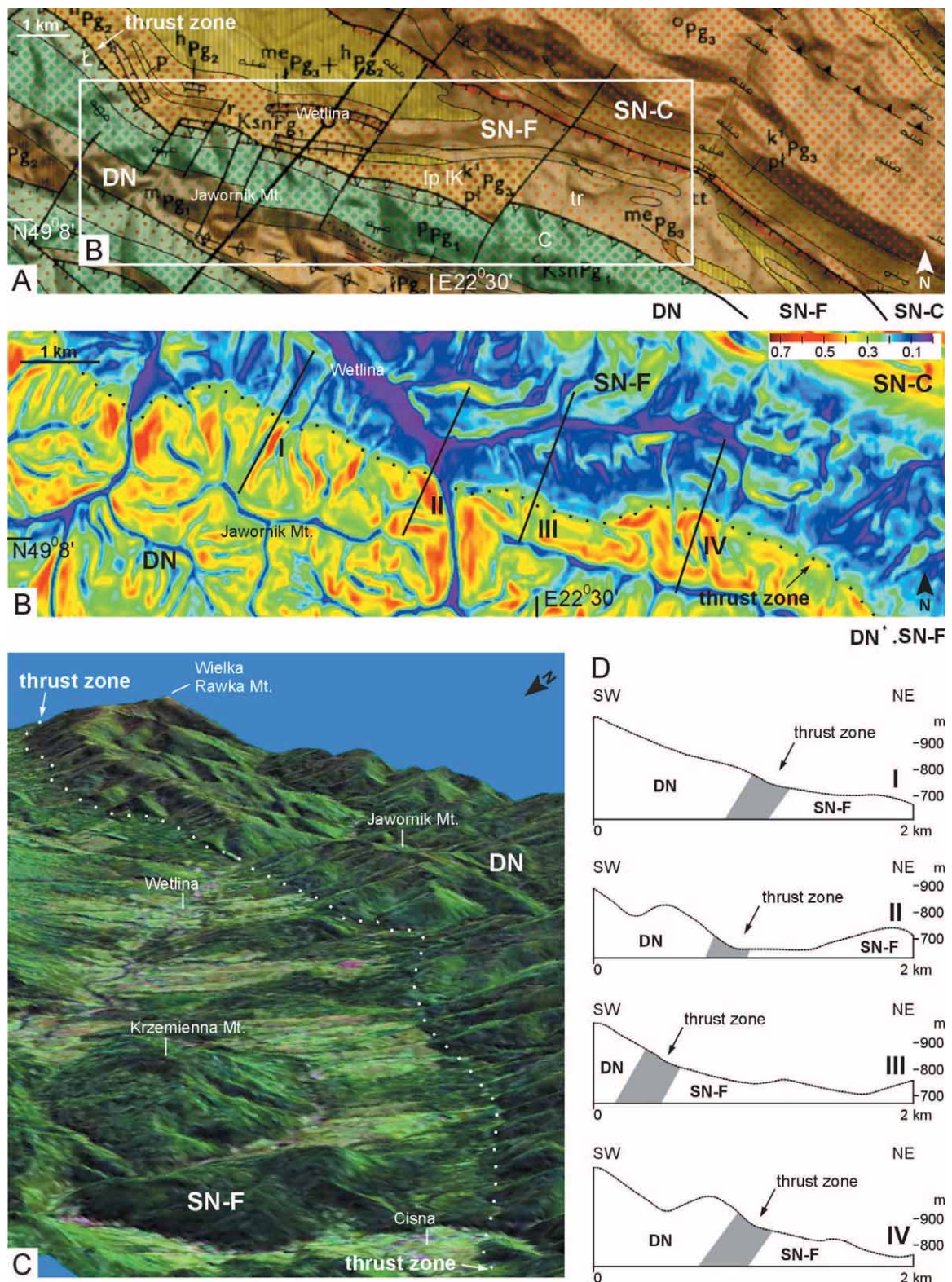
Fig. 10. DEM-products of the Dukla thrust zone in the Wetlina area, DN – Dukla Nappe, SN-F – Silesian Nappe - Foredukla zone, SN-C – Silesian Nappe - Central Carpathian Synclinorium. (A) Geological map (ŚLĄCZKA & ŻYTKO 1979) merged with shaded-relief image (sun direction 45°, sun elevation 60°, 3 × vertical exaggeration). (B) Slope map (values of slopes presented as sine of their angles) with I, II, III, IV elevation profile lines. (C) 3D terrain model of the Dukla thrust zone in the Wetlina area looking east. (D) Elevation profiles (2 × vertical exaggeration) with thrust zone (grey colour). For other explanations see text
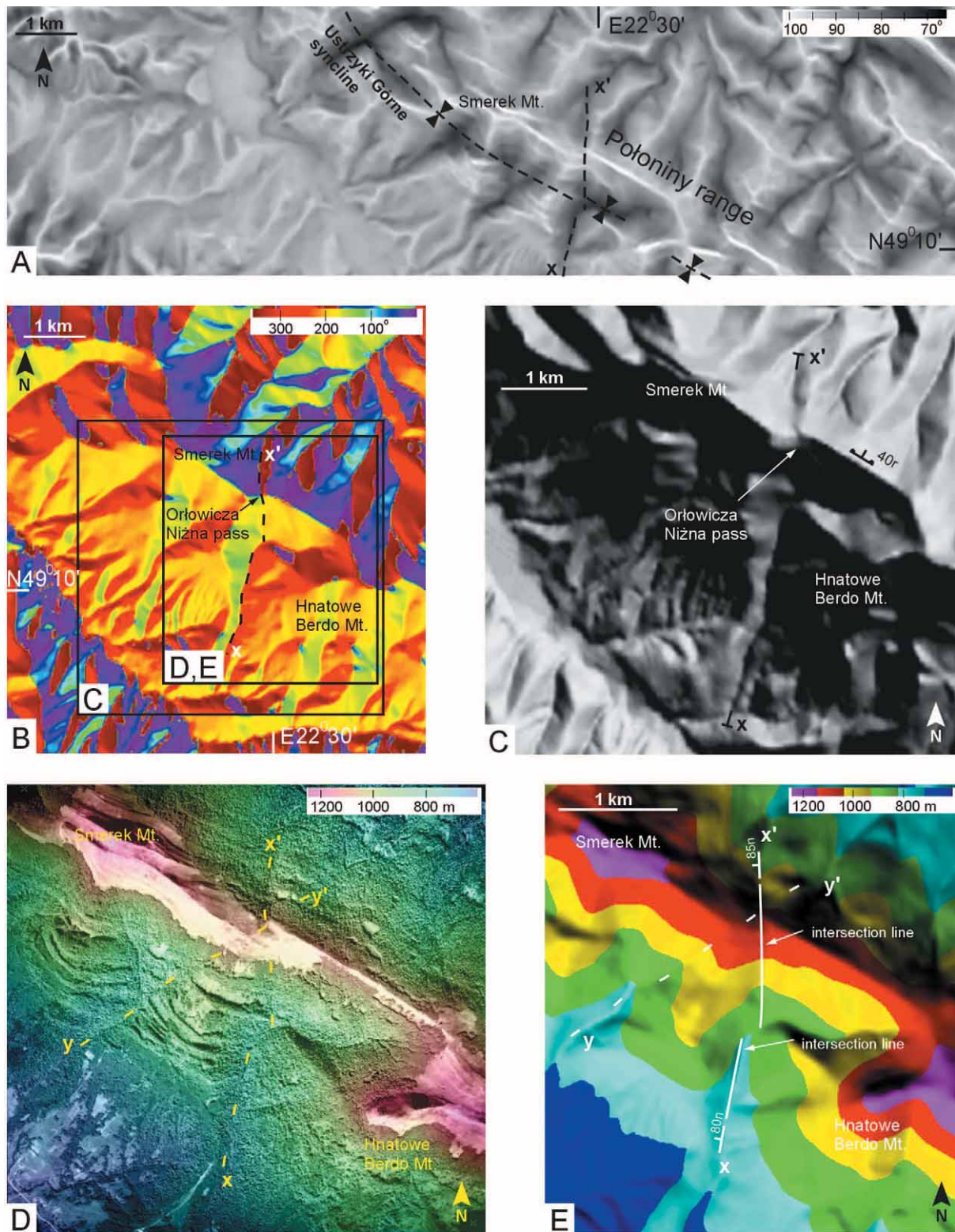
Fig. 11. The DEM derivatives of the Smerek Mt. region. (A) Positive openness map (L = 1000m) with Ustrzyki Górne syncline axis. (B) Aspect map. (C) Shaded-relief image (sun direction 45°, sun elevation 45°, 3 × vertical exaggeration) with bedding orientation (r – reverse); x-x' major fault. (D) Airphoto merged with elevation map; x-x' major fault; y-y' minor fault. (E) Elevation map merged with shaded-relief image (sun direction 225°, sun elevation 45°, 2 × vertical exaggeration) with intersection lines of fault planes and fault orientation (n – normal). For other explanations see text

Aspect, openness, and shaded relief images of this area show that the offset of the ridge is not the effect of intersection between the bedding and terrain surface (Text-figs 11A-C). Probably the offset resulted from movement along the steep-dipping x-x' fault striking at high angles to the ridgeline. Apart from this fault, the trace of the y-y' fault can also be observed (Text-figs 11A, D, E). The offset along this fault is, in contrast, only weakly expressed. The existence of the newly discovered faults is also evidenced by the airphoto of the area, merged with an elevation map (Text-fig. 11D).

The strike and dip of the major x-x' fault have been determined using semiautomatic intersections. The best fit intersection lines suggest that the fault dips generally at 80°-85° to the west and strikes at 0-8° (Text-fig. 11E).

The fault cuts the fold structures and is diagonal to the direction of their shortening. If the fault originally developed as a dextral strike-slip fault, similarly to the majority of the faults with a similar angle relationship to the fold structures (e.g. MASTELLA 1995), it could be reactivated as a sinistral fault or a normal fault with the eastern hanging wall at or after the final stage of folding.

CONCLUSIONS

The application of DEM-derived images, combined with geological maps and satellite images, was found to be useful in discovering faults and recognizing the geometry of folds in the Holy Cross Mountains and the Outer Carpathians in Poland. These DEM derivatives enable the precise identification of faults and determination of their courses, strikes, dips, strike separations and fault movement components. Particularly useful information regarding the general geometry of folds and the spatial distribution of faults is provided by shaded relief images, positive openness maps and 3D terrain images. More precise location of the fault zones and a detailed description of the style of the folds have been possible based on slope and aspects maps, profiling, semiautomatic intersections and contouring.

The analysis has shown that the Łysogóry fault zone is distinctly curvilinear and dominated by series of steeply-dipping faults. The 2 km strike separations across the newly discovered faults which cut the Niewachlów anticline and the prevailing dextral strike-slip components have been estimated. Similarly, across the newly discovered fault which cuts the Połoniny range, the strike-separation of about 200 m and the changing components have been determined. The analysis has demonstrated previously unrecognised changes in the geometry of the Niewachlów anticline, from asymmetric to a fan-shape profile. The applied methods were found to be useful in determining the location of the area of distinct change of vergence of the Baligród syncline. The DEM derivatives have also enabled verification of field observations through determining the course of the Dukla nappe in the Wetlina area and the value of strike separation across the Łysogóry fault.

The analysis has shown that DEM-derived images strongly support structural analysis in the areas where they can be compared with field observations. Such study is also useful in structurally weakly recognized regions.

REFERENCES

ADIYAMAN, O., CHOROWICZ, J. & KÖSE, O. 1998. Relationships between volcanic patterns and neotectonics in Eastern Anatolia from analysis of satellite images and DEM. *Journal of Volcanology and Geothermal Research,* **85**, 17-32.

BANERJEE, S. & MITRA, S. 2005. Fold-thrust styles in the Absaroka thrust sheet, Caribou National Forest area, Idaho-Wyoming thrust belt. *Journal of Structural Geology*, **27**, 51-65.

BERTHELSEN, A. 1993. Where different geological philosophies meet: the Trans-European Suture Zone. *In*: GEE D.G., BECKOLMEN M. (*Eds*), EUROPROBE Symposium Jablonna 1991, *Publications of the Institute of Geophysics, Polish Academy of Sciences*, **255**, 19-31.

BÍL, M. 2003. Spatial (GIS) analysis of relief and lithology of the Vsetínske Vrchy Mountains (Outer West Carpathians, Czech Republic). *Annales Societatis Geologorum Poloniae*, **73**, 55-66.

BOOTH-REA, G., AZAÑÓN, J., AZOR, A. & GARCIA-DUEÑAS, V. 2004. Influence of strike-slip fault segmentation on drainage evolution and topography. A case study: the Palomares Fault Zone (southeastern Betics, Spain). *Journal of Structural Geology*, **26**, 1615-1632.

CHEN, Y., SHYU, J.B.H., OTA, Y., CHEN W., HU J., TSAI B. & WANG Y. 2004. Active structures as deduced from geomorphic features: a case in Hsinchu Area, northwestern Taiwan. *Quaternary International*, **115-116**, 189-199.

COLLET, B., TAUD, H., PARROT, J.F., BONAVIA, F. & CHOROWICZ, J. 2000. A new kinematic approach for the Danakil block using a Digital Elevation Model representation. *Tectonophysics*, **316**, 343-357.

COOPER, G.R.J. 2003. Feature detection using sun shading. *Computers & Geosciences*, **29**, 941-948.

CZARNOCKI, J. 1919. Stratigraphy and tectonics of the Święty Krzyż Mountains. *Prace Towarzystwa Naukowego Warszawskiego*, **28**, 1-172.

— 1938. Carte géologique générale de la Pologne, feuille 4, Kielce, Edition du Service Géologique de Pologne, scale 1:100 000.

— 1950. Geology of the Łysa Góra region (Święty Krzyż Mountains) in connection with the problem of iron ores at Rudki. *Prace Geologiczne Instytutu Geologicznego*, **6a**, 15-400.

— 1956. Surowce mineralne w Górach Świętokrzyskich. *Prace Geologiczne Instytutu Geologicznego,* **5**, 9-108.

— 1957. Tectonics of the Święty Krzyż Mountains. *Prace Geologiczne Instytutu Geologicznego*, **18**, 11-138.

DADLEZ R. & JAROSZEWSKI W. 1994. Tektonika. 743 pp. *Wydawnictwo Naukowe PWN*; Warszawa.

FILONOWICZ, P. 1966. Detailed Geological Map of Poland, Nowa Słupia sheet, scale 1:50 000. *Wydawnictwa Geologiczne*; Warszawa.

— 1968. Explanations to detailed Geological Map of Poland, Nowa Słupia sheet, scale 1:50 000. *Wydawnictwa Geologiczne*; Warszawa.

— 1969. Explanations to detailed Geological Map of Poland, Bodzentyn sheet, scale 1:50 000. *Wydawnictwa Geologiczne*; Warszawa.

— 1973a. Detailed Geological Map of Poland, Kielce sheet, scale 1:50 000. *Wydawnictwa Geologiczne*; Warszawa.

— 1973b. Explanations to detailed Geological Map of Poland, Kielce sheet, scale 1:50 000. *Wydawnictwa Geologiczne*; Warszawa.

FLEMING, M.D. & HOFFER, R.M. 1979. Machine processing of Landsat MSS data and LARS Technical Report 062879. Laboratory for Applications of Remote Sensing, Purdue University, West Lafayette, IN, USA.

FODOR, L., CSONTOS, L., BADA, G., GYÖRFI, I. & BENKOVICS L. 1999. Tertiary Tectonic evolution of the Panonian basin system and neighbouring orogens: a new synthesis of palaeostress data. *In*: DURAND B., JOLIVET L., HORVATH F., SERANNI M. (*Eds*), *The Mediterranean Basins: Tertiary Extension within the Alpine Orogen. Geological Society. London, Special Publications*, **156**, 295-334.

GANAS, A., PAVLIDES, S. & KARASTATHIS V. 2005. DEM-based morphometry of range-front escarpments in Attica, central Greece, and its relation to fault slip rates. *Geomorphology*, **65**, 301-319.

HAKENBERG, M. 1973. The geological map of Poland, Chęciny sheet, scale 1:50 000. *Wydawnictwa Geologiczne*; Warszawa.

HODGSON, M.E. 1998. Comparison of angles from surface slope/aspect algorithms. *Cartography and Geographic Information Systems*, **25**, 173-185.

HOOPER, D.M., BURSIK, M.I. & WEBB, F.H. 2003. Application of high-resolution, interferometric DEMs to geomorphic studies of fault scarps, Fish Lake Valley, Nevada-California, USA. *Remote Sensing of Environment*, **84**, 255-267.

HORN, B.K.P. 1982. Hill shading and the reflectance map. *Geo-Processing*, **2**, 65-146.

IWAHASHI, J., WATANABE, S. & FURUYA, T. 2001. Landform analysis of slope movements using DEM in Higashikubiki area, Japan. *Computers & Geosciences*, **27**, 851-865.

JAROSZEWSKI, W. 1973. Analiza tektonicznych pól naprężeń jako kryterium poszukiwawcze. *Przegląd Geologiczny*, **10**, 523-528. [*In Polish with English summary*]

— 1980. Tektonika uskoków i fałdów, 359 pp. *Wydawnictwa Geologiczne*; Warszawa.

JONES, K.H. 1998. A Comparison of algorithms used to compute hill slope as a property of the DEM. *Computers & Geosciences*, **24**, 315-323.

KIM, Y-S., PEACOCK, D.C.P. & SANDERSON D.J. 2004. Fault damage zones. *Journal of Structural Geology*, **26**, 503-517.

KONON, A., MASTELLA, L. & PIĄTKOWSKA A. 2004. Odwzorowanie struktur tektonicznych starszego podłoża w czwartorzędowej rzeźbie południowo-zachodniej części Gór Świętokrzyskich. *Prace Instytutu Geografii AŚ w Kielcach*, **13**, 33-42.

KSIĄŻKIEWICZ, M. 1972. Budowa geologiczna Polski, t. 4 Tektonika, cz. 3, Karpaty, **4**, **3**, pp. 1-228. *Wydawnictwo Geologiczne*; Warszawa.

KSIĄŻKIEWICZ, M. 1977. The tectonics of the Carpathians. *In:* W. POŻARYSKI (*Ed*.), Tectonics, Geology of Poland, **4**, 476-618. *Instytut Geologiczny*; Warszawa.

KSIĄŻKIEWICZ, M. & SAMSONOWICZ, J. 1953. Zarys geologii Polski, 223 pp. *PWN*; Warszawa.

KSIĄŻKIEWICZ, M., SAMSONOWICZ, J. & RÜHLE, E. 1965. Zarys geologii Polski, 380 pp. *Wydawnictwa Geologiczne*; Warszawa.

KÜHNI, A. & PFIFFNER, O.A. 2001. The relief of the Swiss Alps and adjacent areas and its relation to lithology and structure: topographic analysis from a 250-m DEM. *Geomorphology*, **41**, 285-307.

KUŚMIEREK, J. 1979. Gravitacional deformations and backward overthrusts with reference to deep structures and petroleum prospects of Dukla Unit foreland in the Bieszczady Mountains. *Prace Geologiczne PAN.*, **114**, 1-68. [*In Polish, with English summary*]

LAMARCHE, J., MANSY, J.L., BERGERAT, F., AVERBUCH, O., HAKENBERG, M., LEWANDOWSKI, M., STUPNICKA, E., SWIDROWSKA, J., WAJSPRYCH, B. & WIECZOREK, J. 1999. Variscan tectonics in the Holy Cross Mountains (Poland) and the role of structural inheritance during Alpine tectonics. *Tectonophysics*, **313**, 171-186.

MASTELLA, L. 1995. Tektonika jednostki przeddukielskiej (Bieszczady). Report of the KBN grant No. 600999101.

MILIARESIS, G. & ILIOPOULOU, P. 2004. Clustering of Zagros Ranges from the Globe DEM representation. *International Journal of Applied Earth Observation and Geoinformation*, **5**, 17-28.

MITRA, S. 2003. A unified kinematic model for the evolution of

detachment folds. *Journal of Structural Geology*, **25**, 1659-1673.

MIZERSKI, W. 1982. O zrzutowym charakterze uskoku łysogórskiego. *Biuletyn Geologiczny*, **27**, 193-201. [*In Polish with English summary*]

OGUCHI, T., AOKI, T & MATSUTA, N. 2003. Identication of an active fault in the Japanese Alps from DEM-based hill shading. *Computers & Geosciences*, **29**, 885-891.

OKUBO, C.H., SCHULTZ, R.A. & STEFANELLI G.S. 2004. Gridding Mars Orbiter Laser Altimeter data with GMT: effects of pixel size and interpolation methods on DEM integrity. *Computers & Geosciences*, **30**, 59-72.

ORŁOWSKI, S. 1975. Cambrian and Upper Precambrian lithostratigraphic units in the Holy Cross Mts. *Acta Geologia Polonica*, **25**, 431-446. [*In Polish with English summary*]

OSZCZYPKO, N. 2004. The structural position and tectonosedimentary evolution of the Polish Outer Carpathians. *Przegląd Geologiczny*, **25**, 780-791.

OSZCZYPKO, N. & ŚLĄCZKA, A. 1989. The evolution of the Miocene Basin in the Polish Outer Carpathians and their foreland. *Geologica Carpathica*, **49**, 415-431.

PAWŁOWSKI S. 1965. Zarys budowy geologicznej okolic Chmielnika-Tarnobrzega. *Przegląd Geologiczny*, **6**, 238-245. [*In Polish with English summary*]

PELTON, C. 1987. A computer program for hill-shading digital topographic data sets. *Computers & Geosciences*, **13**, 545-548.

PINIŃSKA, J. 1994. Właściwości wytrzymałościowe i odkształceniowe skał. Skały osadowe regionu świętokrzyskiego, **1/1**, 5-30 pp. Zakład Geomechaniki IHiGI Wydział Geologii Uniwersytetu Warszawskiego. Warszawa.

— 2003. Właściwości wytrzymałościowe i odkształceniowe skał. Skały osadowe regionu świętokrzyskiego, **7**, 5-110 pp. Zakład Geomechaniki IHiGI Wydział Geologii Uniwersytetu Warszawskiego. Warszawa.

PLAŠIENKA, D., GRECULA, P., PUTIŠ, M., KOVÁČ, M. & HOVORKA, D. 1997. Evolution and structure of the Western Carpathians: an overview. *In*: P. GRECULA, D. HOVORKA & M. PUTIŠ (*Eds*), Geological evolution of the Western Carpathians. *Mineralia Slovaca-Monograph*, Bratislava, 1-24i.

POŻARYSKI, W. 1978. The Świętokrzyski Massif. *In*: Geology of Poland, Tectonics, **4**, 216-227pp. *Wydawnictwa Geologiczne*; Warszawa.

RIQUELME, R., MARTINOD, J., HÉRAIL, G. H., DARROZES, J. & CHARRIER R. 2003. A geomorphological approach to determining the Neogene to Recent tectonic deformation in the Coastal Cordillera of northern Chile (Atacama). *Tectonophysics,* **361**, 255- 275.

ROYDEN, L.H. 1988. Late Cenozoic tectonics of the Pannonian Basin System. *AAPG Memoir*, **45**, 27-48.

RUBINKIEWICZ, J. 1996. Tektonika strefy nasunięcia dukielskiego w zachodniej części Bieszczadów. *Przegląd Geologiczny*, **44**, 1199-1204. [*In Polish with English summary*]

SIKORA, W. 1959. Uwagi o stratygrafii i paleografii warstw krośnieńskich na przedpolu Otrytu między Szewczenkiem a Polaną. *Kwartalnik Geologiczny*, **3**, 569-582. [*In Polish with English summary*]

STARKEL, L. 1969. Rozwój rzeźby polskiej części Karpat Wschodnich – na przykładzie dorzecza Górnego Sanu. *Prace geograficzne PAN*, **50**, 1-143. Warszawa.

STUPNICKA, E. 1992. The significance of the Variscan orogeny in the Świętokrzyskie Mountains (Mid-Polish Uplands). *Geologishe Rundschau*, **81**, 561-570.

SUNG, Q. & CHEN, Y. 2004. Geomorphic evidence and kinematic model for quaternary transfer faulting of the Pakuashan anticline, Central Taiwan. *Journal of Asian Earth Sciences*, **24**, 389-404.

ŚLĄCZKA, A. 1971. Geology of the Dukla unit – Polish Flysh Carpathians. *Prace Instytutu Geologicznego*, **63**, 1-167. [*In Polish, with English summary*]

— 1980. Objaśnienia do mapy geologicznej Polski 1:200 000. *Instytut Geologiczny*, 1-53.Warszawa.

ŚLĄCZKA, A. & ŻYTKO, K. 1979. Mapa geologiczna Polski, 1:2000 000, arkusz Łupków. Instytut Geologiczny; Warszawa.

ŚLĄCZKA, A. & KAMIŃSKI, M.A. 1998. A guidebook to excursions in the Polish Flysch Carpathians. Field trips for geoscientists. *Grzybowski Foundation Special Publication,* **6**, 1-167. Kraków.

ŚWIDZIŃSKI, H. 1958. Mapa geologiczna Karpat polskich 1:200 000. Część wschodnia. *Instytut Geologiczny*, Warszawa.

TOKARSKI, A.K., 1975. Geology and geomorphology of the Ustrzyki Górne area. *Studia Geologica Polonica*, **45**, 1-94. [*In Polish, with English summary*]

WALKER, R. & JACKSON, J. 2002. Offset and evolution of the Gowk fault, S.E. Iran: a major intra-continental strike-slip system. *Journal of Structural Geology*, **24**, 1677-1698.

WDOWIARZ, S. 1985. Niektóre zagadnienia budowy geologicznej oraz ropo- i gazonośności centralnego synklinorium Karpat w Polsce. *Biuletyn Instytutu Geologicznego*, **350**, 1-45.

YOELI, P. 1965. Analytical hill shading. *Surveying and Mapping* **25**, 573–579.

YOKOYAMA, R. & *al*. 2002. Visualizing Topography by Opnenness: A New Application of Image Processing to Digital Elevation Models. *Photogrammetric Engineering & Remote Sensing*, **68**, 257-265.

ZHOU, Q. & LIU, X. 2004. Analysis of errors of derived slope and aspect related to DEM data properties. *Computers & Geosciences*, **30**, 369-378.